Progress in Neuropsychopharmacology & Biological Psychiatry 125 (2023) 110760

Contents lists available at ScienceDirect

Progress in Neuropsychopharmacology & Biological Psychiatry

journal homepage: www.elsevier.com/locate/pnp

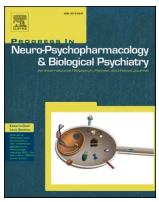

Differential role of GABAergic and cholinergic ventral pallidal neurons in behavioral despair, conditioned fear memory and active coping

Cemal Akmese [1], Cem Sevinc [1], Sahar Halim, Gunes Unal [*]

Behavioral Neuroscience Laboratory, Department of Psychology, Boğaziçi University, 34342 Istanbul, Turkey

ARTICLE INFO

Keywords:
Ventral pallidum
Cholinergic
GABAergic
Behavioral despair
Fear conditioning

ABSTRACT

The ventral pallidum (VP), a major component of the reward circuit, is well-associated with appetitive behaviors. Recent evidence suggests that this basal forebrain nucleus may have an overarching role in affective processing, including behavioral responses to aversive stimuli. We investigated this by utilizing selective immunotoxin lesions and a series of behavioral tests in adult male Wistar rats. We made bilateral GAT1-Saporin, 192-IgG-Saporin or PBS (vehicle) injections into the VP to respectively eliminate GABAergic and cholinergic neurons, and tested the animals in the forced swim test (FST), open field test (OFT), elevated plus maze (EPM), Morris water maze (MWM) and cued fear conditioning. Both GAT1-Saporin and 192-IgG-Saporin injections reduced behavioral despair without altering general locomotor activity. During the acquisition phase of cued fear conditioning, this antidepressant effect was accompanied by reduced freezing and increased darting in the 192-IgG-Saporin group, and increased jumping in the GAT1-Saporin group. In the extinction phase, cholinergic lesions impaired fear memory irrespective of the context, while GABAergic lesions reduced memory durability only during the early phases of extinction in a novel context. In line with this, selective cholinergic, but not GABAergic, lesions impaired spatial memory in the MWM. We observed no consistent effect in anxiety-like behavior assessed in the OFT and EPM. These findings indicate that both the GABAergic and cholinergic neuronal groups of the VP may contribute to emotion regulation through modulation of behavioral despair and acquired fear by suppressing active coping and promoting species-specific passive behaviors.

1. Introduction

The ventral pallidum (VP) is a basal forebrain nucleus acting as a functional interface for translating motivation into motor action (Mogenson et al., 1980). Possessing reciprocal connections with the nucleus accumbens (NAc) and the ventral tegmental area (VTA) (Groenewegen et al., 1993; Haber et al., 1985; Hakan et al., 1992; Heimer et al., 1991; Phillipson and Griffiths, 1985; Root et al., 2015; Taylor et al., 2014; Zahm et al., 1996; Zhou et al., 2022), the VP has been conceptualized as an output station of the dopaminergic mesolimbic pathway (Haber et al., 1985; Pierce and Kumaresan, 2006; Smith et al., 2009), assigning this nucleus a central role in the "reward circuit" of the brain (Haber and Knutson, 2010). Behavioral testing in rodents consistently revealed the involvement of VP in reward processing (Ottenheimer et al., 2020; Richard et al., 2016; Smith et al., 2009; Stephenson-Jones, 2019) as well as hedonic liking (Ho and Berridge, 2013; Smith and Berridge, 2005). In addition to its wide-spread role in appetitive behaviors, the VP may also be involved in regulating responses to aversive stimuli (Cromwell and Berridge, 1993; Wulff et al., 2019; Morais-Silva et al., 2023). Recent evidence suggests that distinct subgroups of VP neurons may contribute to processing of aversive information (Farrell et al., 2021; Moaddab et al., 2021; Saga et al., 2017; Stephenson-Jones et al., 2020). Enhancing VP glutamatergic activity promotes behavioral avoidance (Faget et al., 2018; Stephenson-Jones et al., 2020), while inhibition of VP GABAergic activity leads to heightened risk aversion (Farrell et al., 2021). In addition, non-overlapping parvalbumin (PV)-immunopositive (+) neuronal populations of the VP have been associated with distinct depression-like phenotypes in rodents (Knowland et al., 2017). Following these findings, we elucidate the unique functions of the GABAergic and cholinergic ventral pallidal neurons in behavioral responses to aversive stimuli. We made selective immunotoxin lesions in adult Wistar rats, and tested the animals for behavioral despair, locomotor activity, anxiety-like behavior, spatial learning and conditioned fear memory.

* Corresponding author.
E-mail address: gunes.unal@boun.edu.tr (G. Unal).
[1] Equal contribution.

https://doi.org/10.1016/j.pnpbp.2023.110760
Received 2 February 2023; Received in revised form 24 March 2023; Accepted 6 April 2023
Available online 7 April 2023

Encoding and differentiating appetitive and aversive stimuli are crucial for adaptive behaviors and emotion regulation, while dysfunction in these processes is associated with a wide range of mood disorders (Nusslock and Alloy, 2017). The VP, possessing dense connections with the amygdaloid complex and the prefrontal cortex, plays a central role in valence processing. Co-distributed populations of GABAergic and cholinergic ventral pallidal neurons (Gritti et al., 2006; Gritti et al., 1993) are reciprocally connected with the amygdaloid complex (Agostinelli et al., 2019; Carlsen et al., 1985; Do et al., 2016; Hintiryan et al., 2021; Mascagni and McDonald, 2009; Mcdonald et al., 2011; Záborszky et al., 1984), and provide long-range projections to the prefrontal cortex (Gritti et al., 2003; Henny and Jones, 2008). GABAergic neurons provide approximately 25% of VP projections to the amygdaloid complex (Mascagni and McDonald, 2009), whereas cholinergic neurons comprise almost 75% of these amygdaloid afferents (Carlsen et al., 1985; Woolf and Butcher, 1982). Similar to another basal forebrain projection system, the GABAergic septo-hippocampal pathway (Freund and Antal, 1988; Unal et al., 2015a), approximately 80–90% of the amygdala-targeting VP GABAergic neurons selectively synapse onto GABAergic interneurons in the amygdala (Mcdonald et al., 2011). This suggests that a similar spatio-temporal inhibition mechanism imposed by GABAergic septo-hippocampal projections (Tóth et al., 1997; Unal et al., 2015a, 2018) may exist for the amygdala-targeting VP GABAergic neurons. Ventral pallidal neuronal populations may contribute to the separation of positive and negative valence by modifying local network dynamics of their amygdaloid or prefrontal targets (Espinosa et al., 2019; Záborszky et al., 2018). Considering the anatomical connections between VP neuronal populations and different limbic regions, and the involvement of VP in aversive processing (Moaddab et al., 2021; Wulff et al., 2019), this structure emerges as a key node in neuronal circuitries that process negative affect. However, the role of GABAergic and cholinergic ventral pallidal neurons in behavioral responses to aversive stimuli have not been characterized.

In the current study, we used saporin-based immunotoxins (Bolshakov et al., 2020) to selectively lesion the GABAergic (GAT1-Saporin, selective for GABA transporter type 1 expressing cells) or cholinergic neurons (192-IgG-Saporin, selective for the p75 neurotrophin receptor, colocalized with choline acetyltransferase in the basal forebrain; refer to Batchelor et al., 1989; Dawbarn et al., 1988; Kiss et al., 1988). We performed a battery of behavioral tests to assess alterations in behavioral despair, locomotor activity, anxiety-like behavior, hippocampus-dependent spatial learning, and conditioned fear responses. We found that both GAT1-Saporin and 192-IgG-Saporin injections reduced behavioral despair without altering general locomotor activity. 192-IgG-Saporin group displayed reduced freezing and enhanced active coping during cued fear conditioning, while GABAergic and cholinergic VP neurons differentially contributed to extinction of acquired fear in a context-dependent manner. Similarly, cholinergic, but not GABAergic VP lesions suppressed rearing behaviors in a novel environment and impaired performance in hippocampus-dependent spatial learning.

2. Materials and methods

2.1. Animals

Twenty-seven adult male Wistar rats (240–320 g) were used in the study. Three animals were removed from the experiment prior to behavioral testing due to surgical complications, resulting in a total of 24 rats ($n = 8$ per group). Animals were housed in groups of four under standard vivarium conditions (21 ± 1 °C; ~ 50% humidity; 12:12 day/night cycle with lights on at 8:00 AM) with ad libitum access to food and water. Following stereotaxic surgeries, the animals were transferred to individual cages and remained there until the end of the experiment to minimize the risk of injury around the surgical site, as done in similar studies (see Ahrens et al., 2018; Chang et al., 2017; Doucette et al., 2022). All procedures were approved by the Boğaziçi University Ethics Committee for the Experimental Use of Animals in Scientific Research.

2.2. Stereotaxic surgery

Animals were deeply anesthetized with an IP injection of a mixture of ketamine (85 mg/kg) and xylazine (8.5 mg/kg). Once reflexes were lost, the animals' heads were shaved and they were secured into a stereotaxic frame (Kopf Instruments). Body temperature was kept at approximately 37 °C during the surgery with a heating pad. A local anesthetic (Vemcaine, 10% lidocaine) was applied on the head and a vertical incision was performed to expose the skull. Injection coordinates of the VP (AP = −0.20, ML = ±2.20, DV = −7.60) were determined with reference to the Bregma point according to the rat brain atlas of Paxinos and Watson (2007). Following craniotomy, each animal received bilateral Gat1-Saporin (Advanced Targeting Systems, 325 ng/μl in phosphate buffered saline (PBS), 0.5 μl volume, 0.1 μl/min), 192-IgG-Saporin (Advanced Targeting Systems, 500 ng/μl in PBS, 0.5 μl volume, 0.1 μl/min), or PBS (0.5 μl volume, 0.1 μl/min) injections via 1 μl-Hamilton syringes attached to a microinjection pump (Stoelting). In order to minimize dorsal diffusion, syringes were left in the injection site for five more minutes after the injection was completed. The incision was sutured and local anesthetics (Anestol pomade, 5% lidocaine and Jetokain, 5 mg/kg, SC) and an antiseptic (Batticon) were applied to the stitch.

At the end of the surgery, the animals were taken to the post-operative care unit, placed under an infrared lamp, and monitored until the anesthesia wore off. Each animal went through a 14-day post-surgery recovery period to ensure complete healing and maximize immunotoxin-based elimination of the targeted neuronal populations before behavioral testing began. To facilitate immunohistochemical detection of somatic GABA, four animals from the GAT1-Saporin and vehicle groups underwent a second stereotaxic surgery two weeks after behavioral testing ended and received bilateral colchicine injections into the lateral ventricles. The abovementioned procedures were repeated in these surgeries. Bilateral intracerebroventricular injections of colchicine (50 μg/5 μl in 0.9% saline) were performed using 10 μl-Hamilton syringes.

2.3. Experimental design

Behavioral testing (Fig. 1) started with the 15-minute-long pretest or acclimation session of the forced swim test (FST). Following a 24-hour break, each animal went through the 5-minute test session of the FST. Animals were tested for general locomotor activity in an open field test (OFT) on Day 3 and anxiety-like behavior in an elevated plus maze (EPM) on Day 4. A 5-day Morris water maze (MWM) protocol started on Day 5 and ended with the probe trial on Day 9. We concluded behavioral testing with auditory fear conditioning. Fear acquisition on Day 10 was followed by two extinction sessions on Days 13 and 17. The first session was conducted in the same apparatus as the acquisition, while the second extinction session was conducted in a novel context. In the OFT, EPM and fear conditioning, mazes/chambers were cleaned with 70% ethanol and dried using paper towels between sessions to eliminate olfactory cues for the next animal. Animals underwent perfusion-fixation following behavioral testing ($n = 20$) or colchicine injections ($n = 4$).

2.4. Forced swim test (FST)

We followed the standard FST protocol for rats (Porsolt et al., 1978). Animals were placed into a water-filled cylinder (water depth = 30 cm, temperature = 25 ± 1 °C) and tested twice with a 24-hour break between the pretest (15 min) and test (5 min) sessions. Before each trial, the animal was brought to the behavioral testing room and was allowed to get acclimated to the environment for 5 min. At the end of each trial, the animal was dried with a paper towel, remained under an infrared heating lamp for 30 min and was taken back to its home cage.

Overall duration of immobility, swimming and climbing in the test

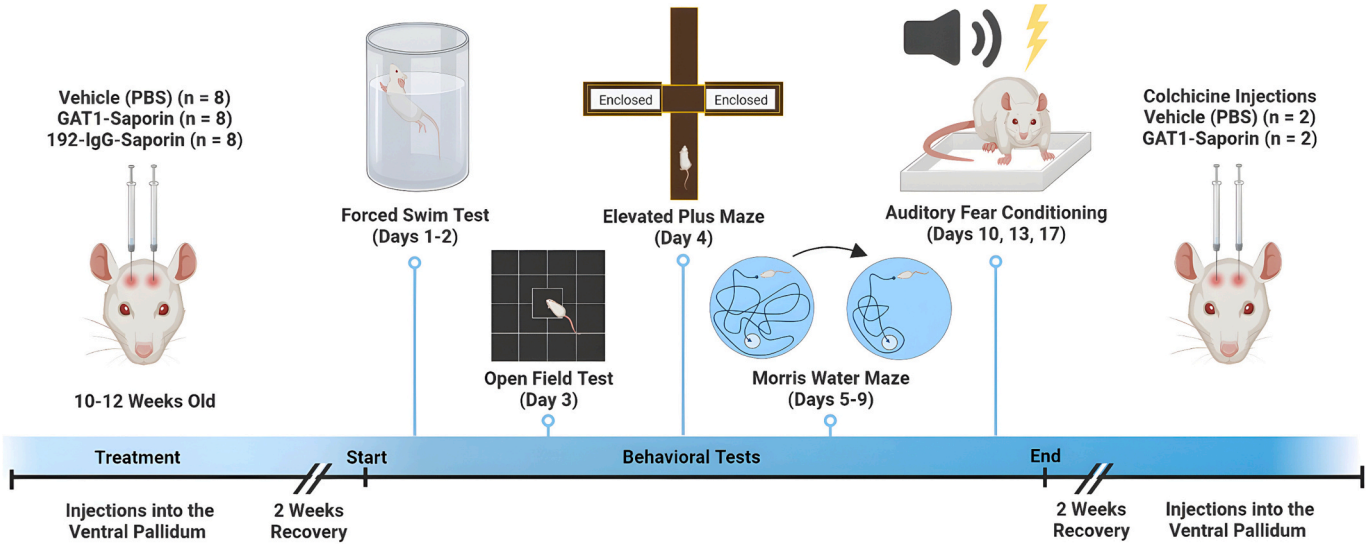

Fig. 1. Experimental timeline illustrating the order of stereotaxic surgeries, recovery periods and the behavioral tests.

session were recorded and analyzed with a time-sampling method (Slattery and Cryan, 2012). The 5-minute session was virtually divided into 5-second bins and the predominant behavior in each bin was determined. Animals were considered immobile when a bin predominantly consisted of passive floating or of any movement that was solely performed to stay above water. Swimming was defined as motor movements parallel to the water surface. Climbing behavior, instead, was operationalized as any active upward-directed motion, during which the animals' forepaws were above the water surface. This is an active response to forced swimming and constitutes a form of active coping. We also recorded the number of headshakes and dives, two common active behaviors in the FST. Bins in which diving or headshaking were the predominant behavior were determined to be climbing behavior. Each animal's behavior was coded by two observers who were blind to the experimental conditions, and the arithmetic means of their scores were used for statistical analyses.

2.5. Open field test (OFT)

Each animal was given a 5-min acclimation period in the test room before the OFT (Gould et al., 2009). They were then placed in an opaque black colored open field (70 × 70 × 45 cm) for 5 min. The time spent in the central area (1600 cm^2) versus periphery (within 15 cm of maze walls), overall locomotion (the average speed and total distance travelled) and the number of rearing behaviors were recorded. Sessions were taped with a video camera and behavioral analyses were performed with a custom DeepLabCut (DLC) (Mathis et al., 2018) implementation.

2.6. Elevated plus maze (EPM)

Anxiety-like behavior was assessed with an EPM positioned 50 cm above the ground (Pellow et al., 1985). It consisted of 2 acrylic transparent (open) and 2 wooden opaque (closed) arms (each arm: 50 × 10 cm). Animals were placed at the center of the maze facing the same open arm. Each session lasted 5 min. The light intensity in different arms were recorded before the session to ensure that illuminance was significantly different in open (120 lx) and closed arms (30 lx). Overall time spent in the open versus closed arms and the number of crossings between the arms were recorded using DLC.

2.7. Morris water maze (MWM)

We used MWM (diameter = 120 cm, water temperature: 21 ± 1 °C) to assess hippocampus-dependent spatial learning and memory (Morris, 1984). The protocol consisted of 4 days of training followed by a single probe trial (Vorhees and Williams, 2006). A circular escape platform (diameter = 10 cm) was placed 2 cm below the water level until it was removed for the probe trial. The water in the maze was opacified with milk powder to obscure the location of the escape platform. Four distinct proximal visual cues, 90° apart, were attached to the walls of the plexiglass maze.

Each training day consisted of four consecutive trials. Animals began each trial from a different starting point. Animals were allowed to stay on the platform for 15 s before being removed from the maze. The maximum amount of time allowed to locate the hidden platform was 2 min. If an animal could not find the platform during this time, it was gently led to the platform by its tail and allowed to stay on the platform for 15 s. Latency to locate the platform (escape latency), average swimming speed, duration spent in each quadrant and the total distance swam were recorded and analyzed in the DLC.

On the probe trial day, the platform was removed from the maze and the animals were tested in a single session for 60 s. We assessed the time spent in the target quadrant where the platform was located during the training days, number of crossings over the original place of the platform, total distance travelled, average speed and thigmotaxis.

2.8. Fear conditioning

We utilized Pavlovian fear conditioning by pairing an auditory conditioned stimulus (CS; 80 dB, 2 kHz, 6 s) with a mild footshock (US; 1.0 mA, 2 s, onset: 0–2 s before CS offset). Delay conditioning carried out on Experimental Day 10 was followed by extinction sessions in the same conditioning chamber (Context A) on Day 13 and in a different box (Context B) on Day 17.

The fear conditioning apparatus (Context A) was a 21 × 45 × 27 cm custom chamber with transparent dark grey acrylic walls. Its floor consisted of 32 metal bars, each 1.4 cm apart, connected to a custom-made stimulator via an Arduino microcontroller. Following a 3-minute baseline measurement phase in the chamber, five CS-US pairings were presented with an intertrial interval (ITI) of 66 s. The extinction sessions consisted of a 3-minute-long baseline measurement followed by 12 presentations of the CS (ITI = 66 s). The second extinction session (Context B) was conducted in a 41 × 43 × 31 cm, open top square chamber with a black solid floor, one transparent and three opaque walls. Context B was also located in a different part of the behavioral testing room, with a different illumination profile. Each session was

conducted under dim light.

All sessions were recorded simultaneously by two video cameras, one positioned above and the other in front of the test chambers. Duration of freezing in response to US or CS presentations, and the number of darting and jumping responses to the US were coded offline by two observers who were blind to the experimental conditions. Darting was operationalized as any sudden acceleration in locomotor activity following shock presentations, barring jumping. Jumping was defined as any motor action, during which none of the four paws of the animal were in contact with the floor. Darting and jumping that happen following footshock (US) or a paired tone (CS) are active responses to aversive stimuli, and constitute active coping mechanisms.

2.9. Histology and immunohistochemistry

Perfusion-fixations were carried out with saline followed by 4% depolymerized paraformaldehyde (PFA) in PBS. Brains were postfixed in PFA for two nights at 4 °C. They were then rinsed in 0.1 M phosphate buffer (PB; 3 × 10 min) and 50–70 μm-thick coronal sections were obtained with a vibrating blade microtome (Leica VT1000 S).

Free-floating immunofluorescence labeling was performed as described by (Unal et al., 2015a). Individual sections were transferred to glass vials and rinsed (3 × 10 min) in PBS containing 0.3% Triton X-100 (PBS-TX) at room temperature (RT). They were immersed in a blocking solution containing 20% normal horse serum (NHS) in PBS-TX for 1 h at RT. The sections were then incubated in primary antibody solutions in PBS-TX with 1% NHS for 48 h at 4 °C. Following primary antibody incubation, the sections were rinsed in PBS-TX (3 × 10 min) and incubated in secondary antibody solutions (PBS-TX with 1% NHS) for 4 h at RT.

We used the following primary antibodies: rabbit anti-parvalbumin (1:2000, ab11427, Abcam), goat anti-choline acetyltransferase (ChAT; 1:500, AB144P, Merck-Millipore), goat anti-ChAT (1:350, ab254118, Abcam), rabbit anti-Leu-enkephalin (Leu-enk; 1:1000, ab22619, Abcam) and rabbit anti-GABA (1:1000, A2052, Sigma). The secondary antibodies were donkey anti-rabbit Alexa Fluor 488 (1:250, ab150073, Abcam) and donkey anti-goat DyLight 650 (1:1000, ab96938, Abcam).

The injection sites (Fig. 2A-B) within the VP were determined by histological verification and immunohistochemistry for Leu-enk (Fig. 2C,E). Standard cresyl violet or DAPI (1:2000, D3571, ThermoFisher; Fig. 2D) staining was utilized in a subset of sections to delineate the borders of basal forebrain nuclei. For DAPI staining, sections were incubated in DAPI solution for 15 min and rinsed in PBS-TX (3 × 10 min) before mounting on glass slides.

Double immunolabeling analyses for PV and ChAT were carried out with 12 randomly chosen brains (n = 4 per group) to determine the specificity and degree of neuronal loss in the VP. Twelve brains (vehicle, n = 4; GAT1-Saporin, n = 4; 192-IgG-Saporin, n = 4) were used for quantifying the degree of GABA-immunoreactive neuronal loss in the ventral pallidum. We quantified the number of PV and ChAT-immunoreactive cell bodies within the VP in 60 randomly selected coronal sections (n = 20 per group). GABA-immunoreactive neuronal somata were located and quantified in 48 randomly selected sections (n = 16 per group).

2.10. Microscopy

An Olympus BX43 epifluorescence microscope was used for observations of injection traces, lesions, and for the quantification of PV, ChAT, or GABA-immunoreactive neuronal bodies (Fig. 2A-B). Images of fluorescent labeling were acquired using the Olympus BX43 epifluorescence microscope, or a Leica SP8 confocal laser scanning microscope equipped with a 20× (Plan Fluotar, N.A. = 0.4, dry, Leica Microsystems)

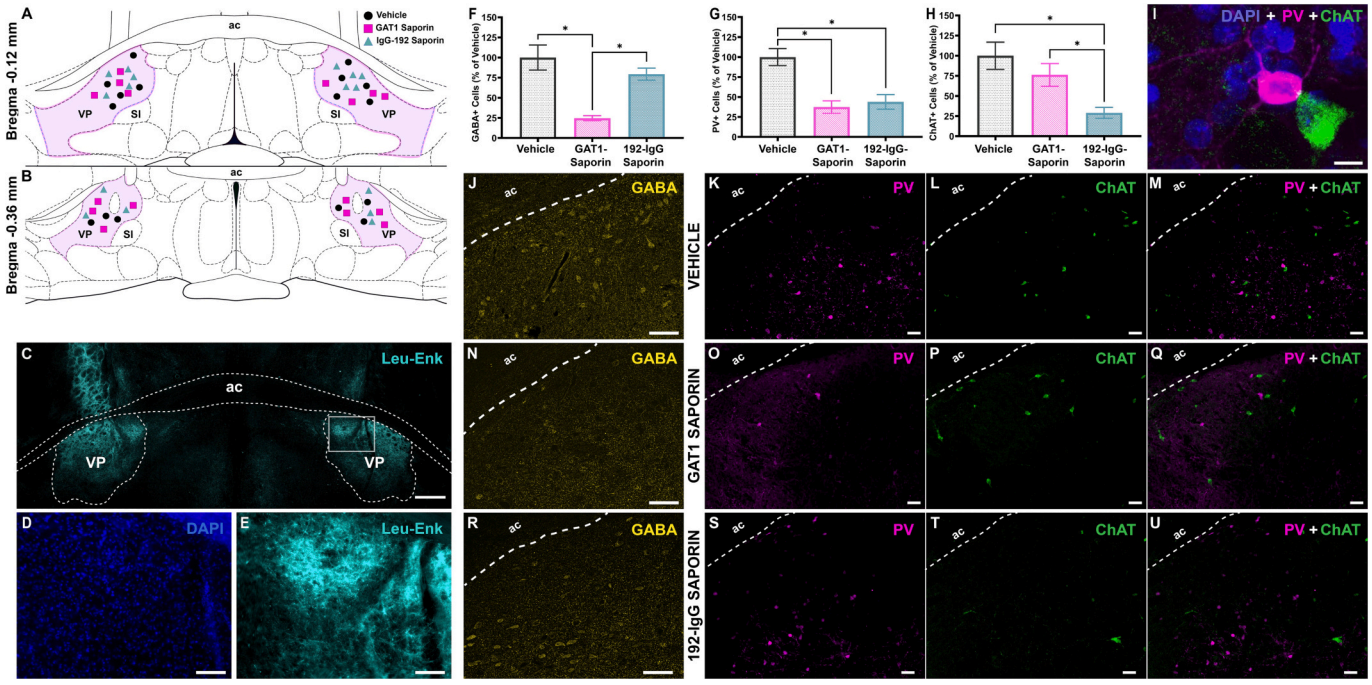

Fig. 2. Histological and immunohistochemical verification of GAT1-Saporin and 192-IgG-Saporin lesions. (A-B) Schematic depiction of coronal sections demonstrating the centers of injection sites (n = 24 animals). (C) Fluorescent immunohistochemistry against Leu-enkephalin showing dense immunopositive fibers in the VP and globus pallidus with relatively sparse labeling in the bed nucleus of stria terminalis and medial preoptic nuclei (scale bar: 500 μm). Higher magnification DAPI (D) and (E) Leu-enkephalin labeling are shown from the rectangular area (scale bars: 100 μm). (F) Average number of GABA+ VP cells per section as a percentage of those in the vehicle group. (G) Average number of PV+ VP cells per section as a percentage of those in the vehicle group. (H) Average number of ChAT+ VP cells per section as a percentage of those in the vehicle group. (I) Maximum intensity projection of a high-power confocal Z-stack in the VP of a vehicle animal showing specific PV and ChAT labeling with a DAPI counterstain (scale bar: 10 μm). (J-R) Representative micrographs demonstrating GABA immunoreactivity in the VP of vehicle (J), GAT1-Saporin (N) and 192-IgG-Saporin (R) animals. (K–U) Representative micrographs depicting double immunohistochemistry for PV and ChAT in the VP of a vehicle (K-M), GAT1-Saporin (O-Q) and 192-IgG-Saporin (S–U) animal. Scale bars (J-U): 50 μm. Error bars show SEM. ac: anterior commissure. * = $p < 0.05$.

and a 40× (Plan Apochromat, N.A. = 1.10, water-immersion, Leica Microsystems) objective lenses. The step size was set at half the optical section thickness for acquisition of z-stacks. Brightness and contrast adjustments of the acquired micrographs were performed uniformly in FIJI (Schindelin et al., 2012). No nonlinear or selective adjustment were made in the acquired images.

2.11. Statistical analysis

All data was tested for normality and sphericity before hypothesis testing. Between-group analyses for normally distributed data were performed by using one-way ANOVAs. Statistically significant main effects were followed by post-hoc comparisons between the vehicle and immunotoxin groups using multiple comparisons with Bonferroni correction. Behavioral tests with multiple trials were analyzed with two-way mixed ANOVAs. When the sphericity assumption was violated, Greenhouse-Geisser correction was used, and the corrected statistics were reported. All statistical analyses were performed with two-tailed tests ($\alpha = 0.05$) using GraphPad Prism version 9.0.0 (GraphPad Software, San Diego, California). All in-text data is presented as mean ± standard deviation (SD). Error bars in figures represent standard error of the mean (SEM).

3. Results

3.1. Selective lesioning

Histological analyses and fluorescent immunohistochemistry were performed on each brain in order to verify the boundaries and effectiveness of immunotoxin injections. The estimated center of each injection site was observed within the boundaries of the VP in both hemispheres (Fig. 2A-B), as delineated by densely labeled Leu-enkephalin-positive processes (Fig. 2C).

Fluorescent immunohistochemistry for GABA, PV, and ChAT produced specific labeling for each neuronal population (Fig. 2I-U). Immunotoxin injections significantly altered the number of GABA-immunopositive (GABA+) ($F(2,9) = 14.77$, $p = 0.0014$, one way ANOVA, Fig. 2F), PV-immunopositive (PV+) ($F(2,9) = 13.930$, $p = 0.0018$, one-way ANOVA; Fig. 2G) and ChAT-immunopositive (ChAT+) neurons ($F(2,9) = 7.382$, $p = 0.0127$, one-way ANOVA; Fig. 2H) in the VP. As there was no difference between the total number of GABAergic cell bodies in colchicine-treated (44.38 ± 29.51) and non-treated brains (51.00 ± 43.63; $t(6) = 0.252$, $p = 0.5371$), subsequent statistical analyses were made by pooling all the sections that have been tested for GABA immunoreactivity.

The proportion of neuronal loss following GAT1- and 192-IgG-saporin injections were in line with previous reports (Dwyer et al., 2007; Pang et al., 2001; Roland et al., 2014; Torres et al., 1994; Yoder and Pang, 2005), Compared to the density of GABA (76.50 ± 23.83) and PV (95.54 ± 20.14) immunoreactivity in the vehicle group, GAT1-Saporin injections led to a significant loss of GABAergic (18.88 ± 4.72; $t(9) = 5.257$, $p = 0.0016$, Bonferroni corrected, Fig. 2F) and PV+ cells (35.71 ± 14.89; $t(9) = 4.801$, $p = 0.0019$, Bonferroni corrected, Fig. 2G) in the VP. The number of GABAergic and PV+ neurons in the VP were respectively reduced by 75% and 63%. No difference was observed in the number of ChAT+ cells (38.46 ± 14.22; $t(9) = 1.264$, $p = 0.4760$, Bonferroni corrected, Fig. 2H) as compared to the vehicle group (50.46 ± 17.03).

192-IgG-Saporin injections caused a significant reduction in the number of both ChAT+ (14.63 ± 6.96; $t(9) = 3.775$, $p = 0.0088$, Bonferroni corrected, Fig. 2F) and PV+ cells (41.96 ± 17.45; $t(9) = 4.300$, $p = 0.0040$, Bonferroni corrected, Fig. 2E), while leaving the overall number of GABAergic neurons unaltered (60.75 ± 11.43; $t(9) = 1.437$, $p = 0.5537$, Bonferroni corrected, Fig. 2D) (Fig. 2F-U). The overall reduction in cholinergic neurons was 71%, while PV+ cells were reduced by 56%.

3.2. Behavioral despair

Immunotoxin administration into the VP significantly altered overall immobility during the second day of the FST ($F(2,21) = 7.564$, $p = 0.0034$, one-way ANOVA; Fig. 3A). Both GAT1-Saporin (64.38 ± 40.19 s, $t(21) = 3.310$, $p = 0.0159$, Bonferroni corrected) and 192-IgG-Saporin (55.63 ± 31.47 s, $t(21) = 3.578$, $p = 0.0053$, Bonferroni corrected) animals displayed reduced immobility compared to the vehicle group (122.5 ± 39.82 s) during FST-2. In contrast, swimming patterns during the test phase of the FST did not change between the groups ($F(2, 21) = 0.665$, $p = 0.5247$, one-way ANOVA; Fig. 3B). Animals in the vehicle (34.69 ± 19.84 s), GAT1-Saporin (30.63 ± 15.45 s) and 192-IgG-Saporin (43.44 ± 30.24 s) groups showed similar levels of swimming.

Both immunotoxin injections increased the duration of climbing behavior ($F(2, 21) = 5.113$, $p = 0.0155$, one-way ANOVA; Fig. 3C) during FST-2. Animals that received intra-VP GAT1-Saporin (205 ± 48.05 s, $t(21) = 2.858$, $p = 0.0282$, Bonferroni corrected) and 192-IgG-Saporin (200.9 ± 37.20 s, $t(21) = 2.671$, $p = 0.0429$, Bonferroni corrected) injections displayed longer periods of climbing compared to the vehicle group (142.8 ± 44.59 s). There were no differences in head-shaking ($F(2, 21) = 0.283$, $p = 0.7561$, one-way ANOVA; Fig. 3D) or diving ($F(2, 21) = 1.382$, $p = 0.2730$, one-way ANOVA) in the FST-2.

3.3. Locomotor activity and anxiety

There was no difference in total distance travelled ($F(2,20) = 1.249$, $p = 0.3082$, one-way ANOVA; Fig. 4A) or in the average speed of locomotion during the OFT ($F(2, 20) = 1.535$, $p = 0.2398$, one-way ANOVA). One animal in the 192-IgG-Saporin group showed excessive freezing in the OFT and did not leave the starting position at the center of the maze (time spent in the center = 300 s vs. group mean = 27.88 ± 24.19 s, z = 11.2513). This outlier was excluded from all OFT analyses.

Saporin injections had a significant effect on the average number of rearing ($F(2,20) = 6.109$, $p = 0.0085$, one way ANOVA, Fig. 4B). 192-IgG-Saporin-injected animals displayed significantly fewer bouts of rearing (13.29 ± 5.53) compared to the GAT-1-Saporin (25.88 ± 10.34, $t(20) = 3.375$, $p = 0.0090$, Bonferroni corrected) animals but not the vehicle group (22.88 ± 3.91, $t(20) = 2.570$, $p = 0.0548$, Bonferroni corrected; Fig. 4B).

There was no difference in anxiety-like behavior observed in the OFT, as assessed by comparing the overall time spent in the central portion of the maze ($F(2, 20) = 0.6952$, $p = 0.5106$, one-way ANOVA; Fig. 4C). Similarly, the percentage of time spent in the open arms of the EPM was not different between the groups ($F(2, 21) = 0.5880$, $p = 0.5643$, one-way ANOVA; Fig. 4D). The number of crossings to open arms did not differ following immunotoxin injections ($F(2, 21) = 1.528$, $p = 0.2401$, one-way ANOVA). All animals showed similar locomotor activity patterns in the OFT, which were dominated by thigmotaxis.

3.4. Spatial learning and memory

MWM analyses revealed a significant decrease in escape latency after four days of training ($F(1.782, 37.43) = 22.78$, $p < 0.0001$, 3 × 4 two-way mixed ANOVA; Fig. 5A), indicating that spatial learning was achieved by the final day of training. We also found a significant main effect of manipulation on the overall time spent to locate the platform ($F(2, 21) = 5.437$, $p = 0.0125$, 3 × 4 two-way mixed ANOVA). The significant difference based on the immunotoxin injections emerged mainly from the impaired spatial navigation performance of the 192-IgG-Saporin animals. 192-IgG-Saporin animals were slower to find the platform on the second ($t(14) = 3.550$, $p = 0.0096$, Bonferroni corrected), and third ($t(9.933) = 3.314$, $p = 0.0237$, Bonferroni corrected) days of training (Fig. 5A) compared to the vehicle group. This was not the case for GAT1-Saporin animals. There was no difference between the escape latencies of GAT1-Saporin and vehicle groups on the first ($t(13.93) = 1.086$, $p = 0.8884$, Bonferroni corrected), second ($t(13.49) = 1.108$, $p = 0.8617$,

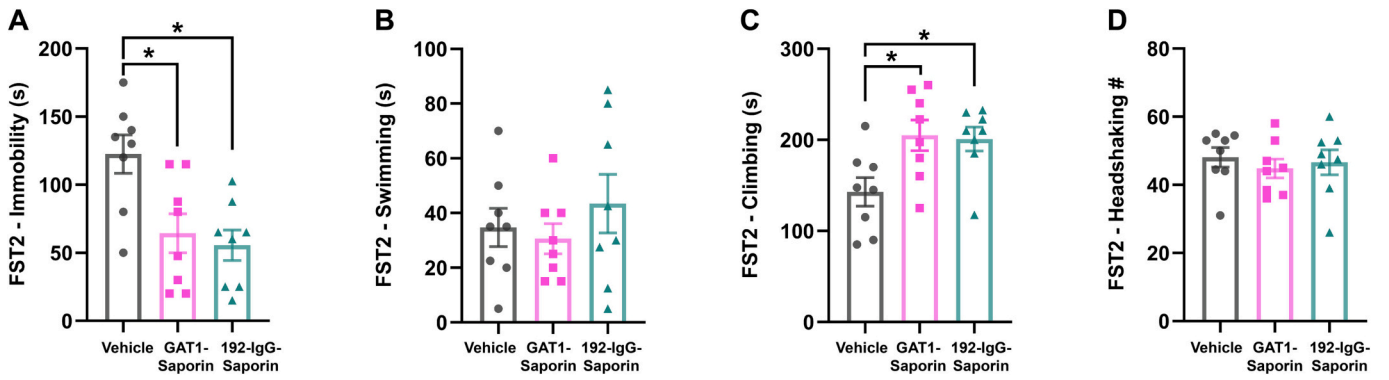

Fig. 3. Behavioral despair analyses from the 5-min test session of the FST. (A-C) Average durations of immobility (A), swimming (B) and climbing/struggling (C). (D) Average number of headshakes. Error bars show SEM. * = $p < 0.05$.

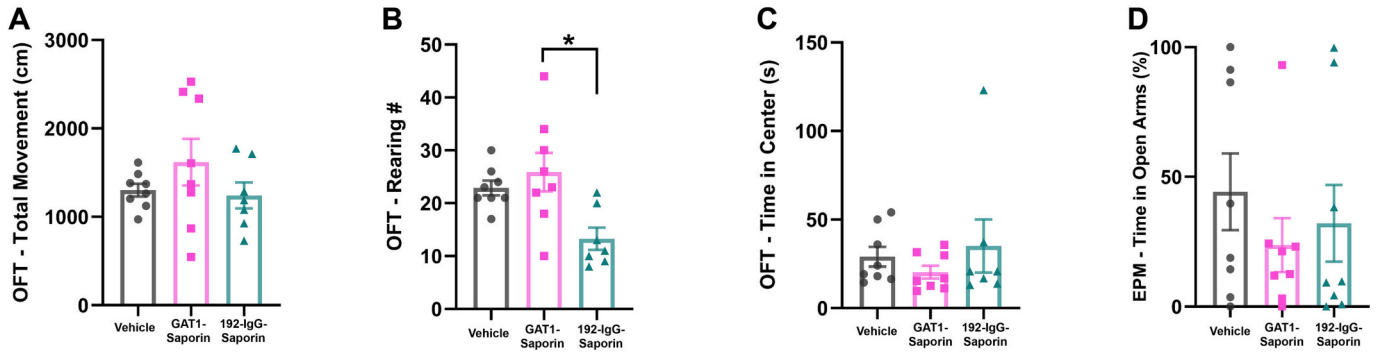

Fig. 4. Assessment of locomotor activity and anxiety-like behavior in the OFT and EPM. (A) Total movement/distance travelled (cm) during the OFT. (B) Average number of rearing performed in the OFT. (C) Average time (s) spent in the central zone of the OFT. (D) Percentage of time spent in the open arms of the EPM. Error bars show SEM. * = $p < 0.05$.

Bonferroni corrected), third ($t(10.69) = 0.6722$, $p > 0.9999$, Bonferroni corrected), or the fourth ($t(11.72) = 0.9400$, $p > 0.9999$, Bonferroni corrected) days of MWM training.

During the probe trial, the groups showed no difference in terms of time spent in the target quadrant ($F(2, 21) = 0.5489$, $p = 0.5857$, one-way ANOVA; Fig. 5B) or the number of platform crossings ($F(2, 21) = 1.812$, $p = 0.1879$, one-way ANOVA; Fig. 5B). The distance travelled ($F(2, 21) = 0.2887$, $p = 0.7522$, one-way ANOVA) or the speed of the animals ($F(2, 21) = 1.622$, $p = 0.2213$, one-way ANOVA) also did not differ between the groups. However, the movement patterns of the groups were significantly different in the probe trial ($F(2, 21) = 6.064$, $p = 0.0083$, one-way ANOVA; Fig. 5C). 192-IgG-Saporin animals (18.96 ± 11.65 s) spent significantly less time in the central zone of the MWM as compared to the vehicle (34.47 ± 11.73 s, $t(21) = 2.750$, $p = 0.360$, Bonferroni corrected) and GAT1-saporin (37.14 ± 10.39 s, $t(21) = 3.225$, $p = 0.0122$, Bonferroni corrected) injected groups during the probe trial. While vehicle injections (Fig. 5D) and GAT1 lesions (Fig. 5E) produced a similar, more distributed swimming pattern, cholinergic lesions lead to predominant thigmotaxis in the probe trial (Fig. 5F).

3.5. Natural and conditioned fear response

Pavlovian fear conditioning to an auditory CS was followed by extinction sessions in the same (Context A) or a different apparatus (Context B), respectively three and seven days after conditioning (Fig. 6A). Immunotoxin injections into the VP altered both the unconditioned and conditioned fear responses. US presentations during fear conditioning led to increased darting behavior in 192-IgG-Saporin (4.50 ± 1.93; $t(21) = 3.114$, $p = 0.0157$, Bonferroni corrected) but not in GAT1-Saporin (4.00 ± 2.00; $t(21) = 2.548$, $p = 0.0562$, Bonferroni corrected) animals compared to the vehicle group (1.75 ± 1.28; $F(2, 21) = 5.504$, $p = 0.0120$, one-way ANOVA; Fig. 6B). The animals also showed an altered frequency of jumping behaviors in response to the US ($F(2, 21) = 13.45$, $p = 0.0002$, one-way ANOVA; Fig. 6C). GAT1-Saporin animals displayed a significantly higher frequency of jumping in response to footshocks (2.13 ± 0.64; $t(21) = 2.954$, $p = 0.0227$, Bonferroni corrected) compared to the vehicle group (1.13 ± 0.83). We found that 192-IgG-Saporin animals (0.38 ± 0.52) jumped significantly less during conditioning compared to the GAT1-saporin injected animals ($t(21) = 5.170$, $p < 0.0001$, Bonferroni corrected) but not the vehicle group ($t(21) = 2.216$, $p = 0.1137$, Bonferroni corrected).

Fear conditioning and extinction sessions started with a 3-min acclimation period, during which baseline freezing was recorded. None of the animals exhibited freezing before conditioning (Fig. 6D). Freezing response emerged with the first CS-US pairing and persistently increased through acquisition trials for all groups ($F(2.032, 42.68) = 10.61$, $p = 0.0002$, 3 × 4 two-way mixed ANOVA; Fig. 6D). Treatment had a significant effect on freezing during the acquisition trials ($F(2, 21) = 3.553$, $p = 0.0469$, 3 × 4 two-way mixed ANOVA; Fig. 6D,H). For further analyses, we binned the triggered responses into two equal blocks for the first and second halves of the fear acquisition and extinction. 192-IgG-Saporin treated animals froze significantly less compared to the vehicle group in the first half ($t(42) = 2.449$, $p = 0.0371$, Bonferroni corrected; Fig. 6H), but not the second half of fear acquisition ($t(42) = 1.954$, $p = 0.1147$, Bonferroni corrected). No difference was observed between the GAT1-saporin and vehicle groups during the earlier ($t(42) = 1.766$, $p = 0.1693$, Bonferroni corrected) or later ($t(42) = 2.092$, $p = 0.0851$, Bonferroni corrected) acquisition trials.

Neither GAT1-Saporin nor 192-IgG-Saporin injections had a significant effect on freezing behavior during the baseline period in the

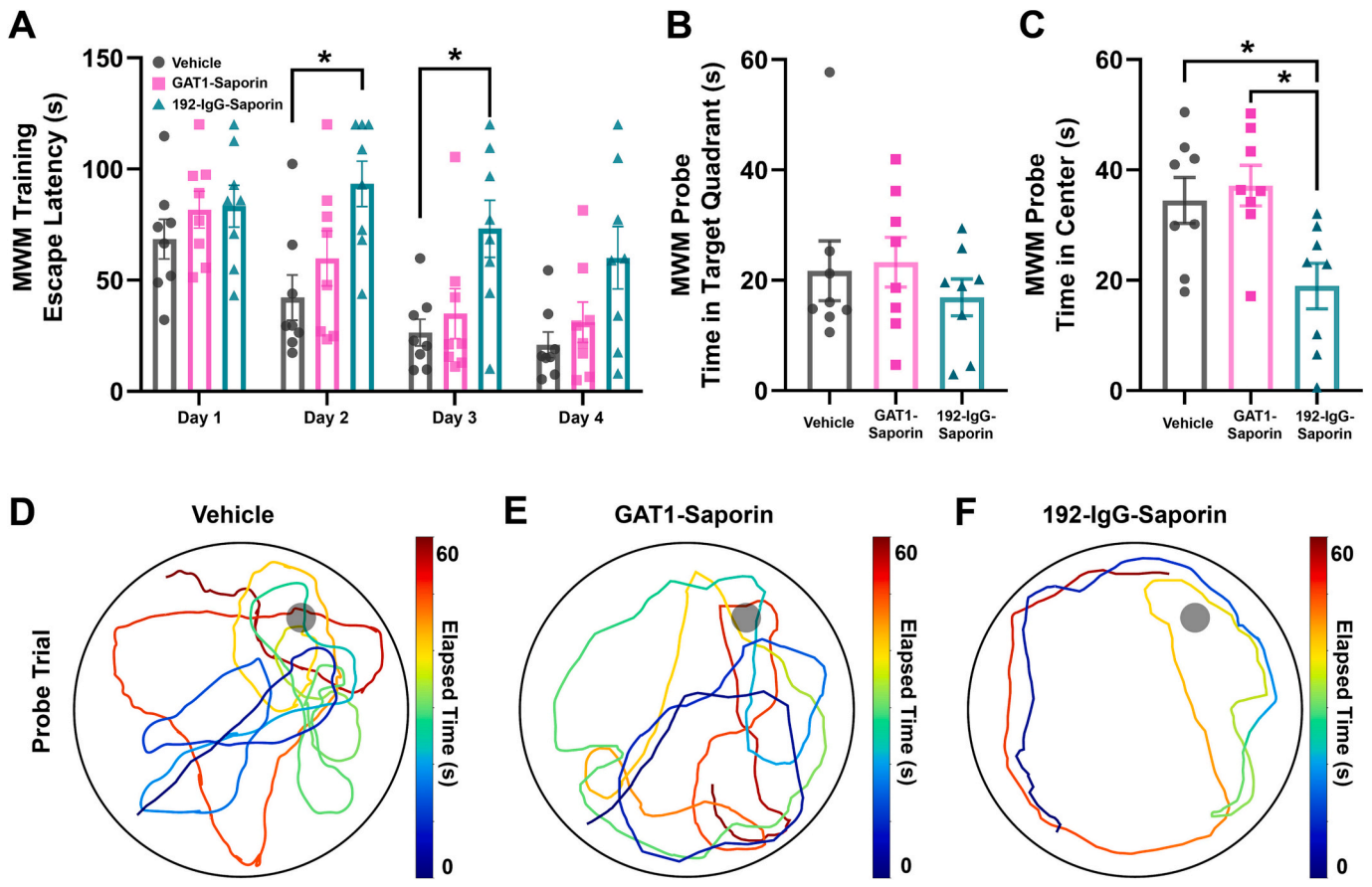

Fig. 5. Spatial learning assessed in the MWM. (A) Average escape latency (s) scores per training day. (B) Average time (s) spent in the target (platform) quadrant during the probe trial. (C) Average time (s) spent in the central area of the MWM during the probe trial. (D-F) Representative swimming trajectories from each group during the probe trial. Error bars show SEM. * = $p < 0.05$.

extinction session conducted in Context A ($F(2, 21) = 0.0746$, $p = 0.9284$, one-way ANOVA; Fig. 6E). Immunotoxin lesions led to altered freezing in the extinction trials in Context A ($F(2, 21) = 8.124$, $p = 0.0024$, 3 × 12 two-way mixed ANOVA) with a significant trial-lesion interaction ($F(22,231) = 2.746$, $p < 0.0001$, 3 × 12 two-way mixed ANOVA; Fig. 6E). Cholinergic lesions significantly reduced freezing throughout the extinction conducted in Context A. This effect was observed during both the first ($t(42) = 2.621$, $p = 0.0243$, Bonferroni corrected; Fig. 6I) and second halves ($t(42) = 3.906$, $p = 0.0007$, Bonferroni corrected) of the Context A trials. There was no statistical difference in freezing between the GABAergic lesion group and the vehicle group during extinction in Context A.

Immunotoxin injections significantly altered freezing behavior during the 3-min baseline period in the extinction test conducted in Context B ($F(2, 21) = 5.319$, $p = 0.0135$, one-way ANOVA; Fig. 6F). Extinction in Context B also revealed a significant effect of experimental manipulation on freezing ($F(2, 21) = 12.32$, $p = 0.0003$, 3 × 12 two-way mixed ANOVA; Fig. 6F). 192-IgG-Saporin lesions caused a reduction in freezing throughout the first ($t(42) = 4.326$, $p = 0.0002$, Bonferroni corrected, Fig. 6J) as well as the second ($t(42) = 4.840$, $p < 0.0001$, Bonferroni corrected) half of extinction in the novel context, as compared to the vehicle group. In the novel context, GAT1-Saporin animals (36.81 ± 14.24) also showed significantly less freezing in the first 6 trials compared to the vehicle group (51.52 ± 11.03; $t(42) = 2.373$, $p = 0.0446$, Bonferroni corrected, Fig. 6J). The reduction in freezing observed in the first half of novel context extinction following GABAergic VP lesions did not persist in the second half ($t(42) = 1.909$, $p = 0.1263$, Bonferroni corrected). While 192-IgG-Saporin injections led to an overall impairment of conditioned fear memory, performance decrease in the GAT1-Saporin group was restricted to the early phase when context-related cues were missing.

Exploratory correlation analyses across groups revealed correlations between several measures of passive coping (Fig. 6G). We found significant correlations between the average duration of freezing during fear acquisition and extinction in Context A ($r(22) = 0.489$, $p = 0.015$) as well as in Context B ($r(22) = 0.449$, $p = 0.028$). The two extinction sessions were also correlated with each other ($r(22) = 0.731$, $p < 0.001$). There was a significant correlation between immobility duration in the second FST session and the freezing responses in Context B extinction ($r(22) = 0.481$, $p = 0.017$). The groups formed distinct clusters in the exploratory space when we mapped individual freezing responses during fear acquisition and extinction in the novel context (Fig. 6K). The vehicle group showed high levels of freezing with relatively low variability both during fear conditioning and Context B extinction. The 192-IgG-Saporin group was characterized by significantly lower levels of cued freezing, while the freezing scores of GAT1-Saporin animals were distributed between the other two groups (Fig. 6K).

4. Discussion

We showed that selective GABAergic or cholinergic VP lesions led to altered behavior in distinct affective and cognitive processes. GAT1-Saporin lesions selectively reduced the number of PV+ and GABA+ VP neurons, while sparing ChAT+ neurons. 192-IgG-lesions, in contrast, caused a decrease in the number of ChAT+ and PV+ VP neurons, but did not change the overall number of GABA-immunoreactive neurons in the VP, as previously shown by Torres et al. (1994). Both lesions led to an

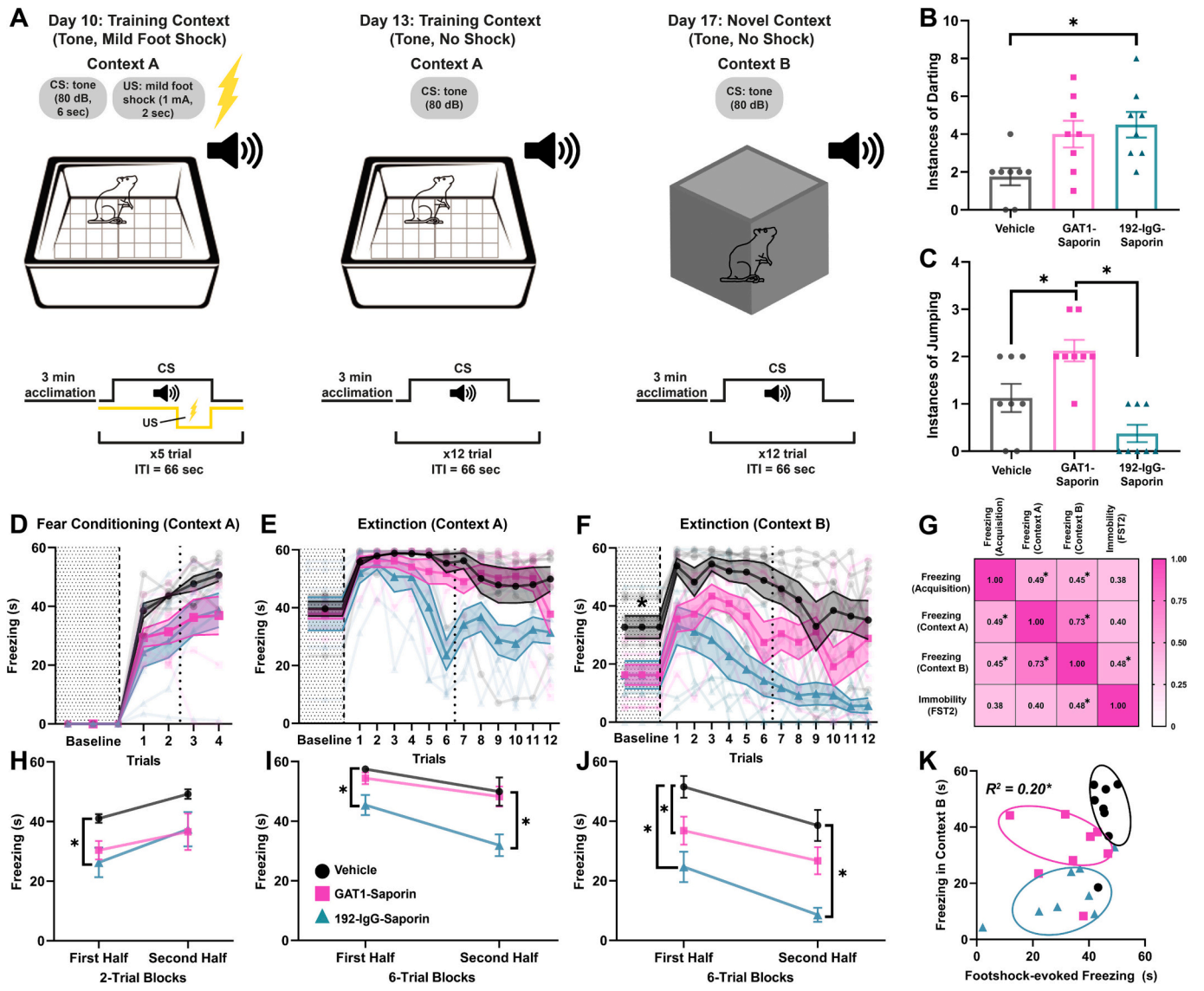

Fig. 6. Auditory fear conditioning. (A) Schematic depiction of pairing and extinction sessions. (B–C) Instances of darting (B) and jumping (C) in response to footshock. (D–F) Freezing during fear conditioning (D), extinction in the conditioning apparatus (Context A) (E) and extinction in a novel apparatus (Context B) (F). Dashed lines in D–F demarcate the baseline and dotted lines separate the first and second halves of the session. (G) Correlation matrix of passive coping: freezing during fear acquisition, freezing during extinction in Context A, freezing during extinction in Context B, and immobility in FST-2. (H-J) Freezing during the first and second halves of fear acquisition (H), extinction in the same context (I) and extinction in a novel context (J). (K) Scatter plot of the correlation between average footshock-evoked freezing and freezing in Context B. The distinct clusters formed by the three groups are encircled. Error bars show SEM. * = $p < 0.05$.

overall increase in the frequency of active responses to aversive stimuli, namely climbing in the FST, and darting or jumping in response to mild footshocks. A substantial reduction in behavioral despair and higher levels of active coping were observed in both groups. Immunotoxin injections led to differential effects in fear responses during the acquisition and extinction sessions of cued fear conditioning. Cholinergic lesions impaired freezing during the early phase of acquisition and led to increased darting in response to mild footshocks. 192-IgG-Saporin-injected animals also showed impaired retention of fear memory throughout both extinction sessions. GABAergic lesions, however, only altered freezing in the early stages of Context B extinction, indicating that GABAergic VP neurons were required for the durability of fear memory selectively in the early phases of extinction when the context information was missing. The differential role of cholinergic and GABAergic VP neurons in context-dependent behavior extended to other cognitive functions as 192-IgG-Saporin caused suppressed rearing, an indication of exploratory behavior, and impaired spatial long-term memory. We observed relatively high levels of within-group variability in the EPM, and did not find an immunotoxin-induced change in anxiety-like behavior.

Ventral pallidum is a core component of the reward and motivation circuitry of the mammalian brain, with well-known functions in motivated and appetitive behaviors (Ottenheimer et al., 2020; Root et al., 2015). However, its role in aversive processing has only recently attracted scientific attention (Farrell et al., 2021; Moaddab et al., 2021; Saga et al., 2017; Stephenson-Jones et al., 2020). We investigated this relatively understudied system by lesioning the GABAergic and cholinergic populations of the VP, and revealed that both neuronal groups contribute to behavioral despair and conditioned fear responses by suppressing active coping. Climbing, or struggling in the FST chamber, and darting and jumping responses to footshock in fear conditioning constitute active responses to aversive stimuli (i.e. active coping). Our observations on these active coping mechanisms corroborate existing electrophysiological (Moaddab et al., 2021) and behavioral evidence

(Saga et al., 2017), pointing to a crucial role for VP GABAergic neurons in producing adaptive emotional responses to aversive stimuli.

4.1. Depression-like behavior

The VP has reciprocal connections with several brain regions that are directly implicated depression-like behaviors in rodents. These include the nucleus accumbens, lateral habenula, ventral tegmental area, amygdaloid complex, and prefrontal cortex (Gielow and Zaborszky, 2017; Groenewegen et al., 1993; Haber et al., 1985; Hakan et al., 1992; Heimer et al., 1991; Phillipson and Griffiths, 1985; Root et al., 2015; Taylor et al., 2014; Zahm et al., 1996). Despite these connections, the role of VP in affective disorders has largely been neglected (Root et al., 2015). Here, we found that selective deletion of GABAergic or cholinergic VP neurons produced potent antidepressant-like effects in the FST.

It is important to note the FST, the most common behavioral rodent test of antidepressant efficacy, has been criticized for its construct validity (Molendijk and de Kloet, 2015, 2019). The main measure of this test is immobility, which corresponds to the rodent endophenotype of psychomotor retardation, a symptom required for clinical diagnosis of major depressive disorder (American Psychiatric Association, 2013; Unal and Canbeyli, 2019). In the current study, both lesion groups had decreased immobility in the test phase. In line with this, we found a significant increase in active climbing behavior (i.e. struggling). Differences in the FST analyses did not arise from different levels of general locomotor activity between the groups as the OFT results revealed similar activity levels for all animals. Post-surgical individual housing of the animals, however, may have influenced the FST results. Social isolation is a common rodent model of stress (Djordjevic et al., 2012; Unal, 2021), which often heightens anxiety levels and leads to depression-like behaviors following short (Takatsu-Coleman et al., 2013) or chronic (Djordjevic et al., 2012) exposure. Since VP is suggested to be involved in the anxiogenic and depressogenic effects of social isolation (Lehr, 2022), it is important to consider the potential effects of individual housing in the current findings.

Heightened VP GABAergic tone leads to increased immobility during the test phase of the FST, while bilateral intra-VP bicuculline injections produce antidepressant-like effects (Skirzewski et al., 2011). Approximately 90% of PV+ neurons in the basal forebrain synthesize glutamic acid decarboxylase, the synthetic enzyme for GABA (Gritti et al., 2003). Two parallel projections of distinct PV+ subpopulations of the VP target the lateral habenula or VTA and differentially contribute to different depression-like rodent endophenotypes (Knowland et al., 2017). Interestingly, Knowland et al. (2017) showed that a substantial portion of the PV+ projection neurons in the VP may be glutamatergic. This may partially explain our observations and previous findings (Torres et al., 1994) showing that IgG-192-Saporin lesions decrease the number of PV+ but not GABA+ neurons in the basal forebrain. The VP also contributes to stress-induced depression-like behavior by suppressing dopaminergic activity through its connections with the basolateral amygdala (BLA) (Chang and Grace, 2014). Supporting earlier findings regarding the role of VP GABAergic neurons in depression-like behaviors, our results provide the first direct functional evidence for the involvement of VP GABAergic neurons in behavioral despair.

Furthermore, we showed that selective lesioning of cholinergic neurons in the VP leads to antidepressant-like effects. The role of the cholinergic system in regulating depressive symptoms has previously been tested by pharmacological manipulations in the basal forebrain or their target structures (Dulawa and Janowsky, 2019). Systemic injections of acetylcholinesterase inhibitors into the VTA or hippocampus (Addy et al., 2015; Mineur et al., 2013; Small et al., 2016) as well as intra-VTA, or intra-NAc injections of cholinergic receptor agonists (Andreasen and Redrobe, 2009; Chau et al., 2001; Haj-Mirzaian et al., 2015; Small et al., 2016) produce depression-like outcomes. In contrast, muscarinic or nicotinic antagonists lead to antidepressant-like effects (Aboul-Fotouh, 2015; Addy et al., 2015; Chau et al., 2001; Ghosal et al., 2018; Haj-Mirzaian et al., 2015; Navarria et al., 2015). Moreover, cholinergic innervation of the ventral subiculum leads to depression-like behavior which may be reversed by atropine injections (Yu et al., 2022). Here, we show that the antidepressant effects of suppressing or silencing the cholinergic system extend to the VP. It is likely that cholinergic neurons that localize in different basal forebrain subnuclei target distinct limbic regions and contribute to different depression-like phenotypes (Unal and Moustafa, 2021).

We observed an increase in climbing but not swimming following VP lesions. Similar climbing-specific alterations that spare swimming performance was observed following administration of selective norepinephrine reuptake inhibitors (Cryan et al., 2002, 2005; Detke et al., 1995). Basal forebrain GABAergic and cholinergic neurons express noradrenergic receptors and receive noradrenergic input (Root et al., 2015; Schwarz and Luo, 2015; Watson et al., 2012), while the VP provides sparse projections back to the locus coeruleus (Groenewegen et al., 1993). These behavioral and anatomical findings suggest that lesioning VP cholinergic or GABAergic neuronal populations may have led to alterations in noradrenergic signaling pathways that selectively alter climbing behavior, but not swimming in the FST.

4.2. Conditioned fear memory and active coping

Baseline recordings showed no freezing in any of the animals prior to presentation of the first footshock (US). Interestingly, the vehicle group displayed significantly higher freezing to the first CS-US pairing compared to the 192-IgG-Saporin group (Fig. 6D,H). As this was the very first presentation of the footshock, it showed that selective deletion of VP cholinergic neurons altered the unconditioned, or natural, response to an aversive stimulus. This was accompanied by enhanced darting responses in the cholinergic lesion group and increased shock-triggered jumping in the GAT1-Saporin animals during fear acquisition, suggesting behavior-specific alterations in active coping following GABAergic or cholinergic lesions. Diminished unconditioned freezing observed in the cholinergic group did not persist for the whole acquisition (Fig. 6D, H). Cholinergic, but not GABAergic lesions impaired context-dependent fear memory during the same-context session. It is important to note that the significant difference in freezing was manifested starting with the sixth trial. For this reason, it is also possible to argue that VP cholinergic lesions do not impair acquired fear memory, but instead lead to enhanced extinction learning (Knox, 2016; Wilson and Fadel, 2017). In the novel context, both GABAergic and cholinergic lesions reduced durability of the fear memory during the early phases of extinction. This effect persisted in the second half of the session only for the 192-IgG-Saporin group. There was no difference between the GAT1-Saporin and control animals in the second half of the novel context extinction.

Cholinergic inputs to BLA increase signal-to-noise ratio (Unal et al., 2015b) and modulate the durability of fear memories (Crimmins et al., 2022). Systemic applications of cholinergic antagonists lead to decreased freezing during fear acquisition (Anagnostaras et al., 1999; Figueredo et al., 2008; Fornari et al., 2000; Soares et al., 2006), cause memory deficits in context conditioning (Anagnostaras et al., 1995; Figueredo et al., 2008; Fornari et al., 2000), cued fear conditioning (Young et al., 1995), or both context and cued conditioning (Anagnostaras et al., 1999; Feiro and Gould, 2005; Rudy, 1996). Paralleling our findings, high doses of scopolamine (Anagnostaras et al., 1999) or inhibition of basal forebrain cholinergic terminals in the BLA (Jiang et al., 2016) eliminate freezing during fear acquisition without altering pain sensitivity. Inhibition of VP GAD1 neurons alter the motivation to avoid an aversive stimulus, but does not alter shock reactivity (Farrell et al., 2021). Similarly, we show that selective cholinergic lesions led to enhanced darting behavior during fear acquisition, but, unlike GABAergic lesions, did not increase the number of US-driven jumping behavior.

Baseline recordings of the extinction session in the novel context indicate that the vehicle group could generalize the context information

of the cued conditioning (Fig. 6F). This was contrasted by both immunotoxin groups showing diminished baseline freezing in the novel context. Both groups also showed less conditioned freezing in the earlier phases of the extinction session in the novel context. The memory impairment led by VP cholinergic lesions was sustained across different paradigms (i.e. MWM and cued fear conditioning) and contexts. Hence, VP cholinergic lesions may have led to alterations in hippocampal circuitry that result in a general hippocampus-dependent memory impairment. In contrast, the effects of GABAergic lesions were specific to the early phases of extinction in a novel context, suggesting a specific disruption in conditioned fear memory. The differences observed in active coping and conditioned freezing altogether suggest differential roles for the GABAergic and cholinergic VP neurons in natural (i.e. spontaneous) responses to aversive stimuli. Moreover, GABAergic VP lesions led to antidepressant-like and active-coping-promoting effects without impairing exploratory rearing behaviors, long-term spatial memory, or context-dependent fear memory.

The revealed role of VP GABAergic neurons in behavioral despair and fear memory possibly arises via their connections to the amygdaloid circuitry (Mascagni and McDonald, 2009; McDonald et al., 2012; Mcdonald et al., 2011). GABAergic neurons of the VP regulate BLA-dependent phenomena such as the prepulse inhibition of acoustic startle (Kodsi and Swerdlow, 1997; Kodsi and Swerdlow, 1995; Swerdlow et al., 1990). Bilateral muscimol injections into the VP following BLA inactivation restores prepulse inhibition to normal levels (Forcelli et al., 2012). Long-range GABAergic projections of the VP may accordingly function as a mediator for amygdala-dependent acquired behaviors.

5. Conclusion

The present study provided direct evidence for the involvement of VP in behavioral responses to aversive stimuli. We show that the GABAergic and cholinergic neuronal populations of the VP contribute to depression-like phenotypes, unconditioned fear responses and distinct memory processes. Selective lesioning of these neuronal groups produced antidepressant effects and increased active coping, while differentially reducing the durability of fear memories. VP cholinergic lesions impaired memory across all stages of MWM and cued fear conditioning, while GABAergic lesions selectively impaired memory performance during extinction in a novel context. These findings suggest that the GABAergic and cholinergic neuronal groups of the VP may constitute separate but complementary therapeutic targets for treatment of mood disorders.

Funding

This research was funded by an EMBO Installation Grant (no: 4432) to GU.

CRediT authorship contribution statement

Cemal Akmese: Methodology, Investigation, Writing – original draft. **Cem Sevinc:** Methodology, Investigation, Writing – original draft. **Sahar Halim:** Methodology, Investigation, Writing – original draft. **Gunes Unal:** Conceptualization, Methodology, Project administration, Funding acquisition, Writing – review & editing.

Declaration of Competing Interest

The authors declare that there is no conflict of interest.

Data availability

Data will be made available on request.

References

Aboul-Fotouh, S., 2015. Behavioral effects of nicotinic antagonist mecamylamine in a rat model of depression: prefrontal cortex level of BDNF protein and monoaminergic neurotransmitters. Psychopharmacology 232, 1095–1105. https://doi.org/10.1007/S00213-014-3745-5.

Addy, N.A., Nunes, E.J., Wickham, R.J., 2015. Ventral tegmental area cholinergic mechanisms mediate behavioral responses in the forced swim test. Behav. Brain Res. 288, 54. https://doi.org/10.1016/J.BBR.2015.04.002.

Agostinelli, L.J., Geerling, J.C., Scammell, T.E., 2019. Basal forebrain subcortical projections. Brain Struct. Funct. 224, 1097–1117. https://doi.org/10.1007/s00429-018-01820-6.

Ahrens, A.M., Ferguson, L.M., Robinson, T.E., Aldridge, J.W., 2018. Dynamic encoding of incentive salience in the ventral pallidum: dependence on the form of the reward cue. eNeuro 5. https://doi.org/10.1523/ENEURO.0328-17.2018. ENEURO.0328-17.2018.

American Psychiatric Association, 2013. Diagnostic and statistical manual of mental disorders. Am. Psychiat. Assoc. https://doi.org/10.1176/appi.books.9780890425596.

Anagnostaras, S.G., Maren, S., Fanselow, M.S., 1995. Scopolamine selectively disrupts the acquisition of contextual fear conditioning in rats. Neurobiol. Learn. Mem. 64, 191–194. https://doi.org/10.1006/NLME.1995.0001.

Anagnostaras, S.G., Maren, S., Sage, J.R., Goodrich, S., Fanselow, M.S., 1999. Scopolamine and pavlovian fear conditioning in rats: dose-effect analysis. Neuropsychopharmacology 21 (6), 731–744. https://doi.org/10.1016/s0893-133x(99)00083-4.

Andreasen, J.T., Redrobe, J.P., 2009. Antidepressant-like effects of nicotine and mecamylamine in the mouse forced swim and tail suspension tests: Role of strain, test and sex. Behav. Pharmacol. 20, 286–295. https://doi.org/10.1097/FBP.0B013E32832C713E.

Batchelor, P.E., Armstrong, D.M., Blaker, S.N., Gage, F.H., 1989. Nerve growth factor receptor and choline acetyltransferase colocalization in neurons within the rat forebrain: response to fimbria-fornix transection. J. Comp. Neurol. 284, 187–204. https://doi.org/10.1002/cne.902840204.

Bolshakov, A.P., Stepanichev, M.Y., Dobryakova, Y.V., Spivak, Y.S., Markevich, V.A., 2020. Saporin from saponaria officinalis as a tool for experimental research, modeling, and therapy in neuroscience. Toxins (Basel) 12. https://doi.org/10.3390/TOXINS12090546.

Carlsen, J., Záborszky, L., Heimer, L., 1985. Cholinergic projections from the basal forebrain to the basolateral amygdaloid complex: a combined retrograde fluorescent and immunohistochemical study. J. Comp. Neurol. 234, 155–167. https://doi.org/10.1002/cne.902340203.

Chang, C.H., Grace, A.A., 2014. Amygdala-ventral pallidum pathway decreases dopamine activity following chronic mild stress in rats. Biol. Psychiatry 76, 223. https://doi.org/10.1016/J.BIOPSYCH.2013.09.020.

Chang, S.E., Smedley, E.B., Stansfield, K.J., Stott, J.J., Smith, K.S., 2017. Optogenetic inhibition of ventral pallidum neurons impairs context-driven salt seeking. J. Neurosci. 37, 5670. https://doi.org/10.1523/JNEUROSCI.2968-16.2017.

Chau, D.T., Rada, P., Kosloff, R.A., Taylor, J.L., Hoebel, B.G., 2001. Nucleus accumbens muscarinic receptors in the control of behavioral depression: antidepressant-like effects of local M1 antagonist in the Porsolt swim test. Neuroscience 104, 791–798. https://doi.org/10.1016/S0306-4522(01)00133-6.

Crimmins, B.E., Lingawi, N.W., Chieng, B.C., Leung, B.K., Maren, S., Laurent, V., 2022. Basal forebrain cholinergic signaling in the basolateral amygdala promotes strength and durability of fear memories. Neuropsychopharmacology 2022, 1–10. https://doi.org/10.1038/s41386-022-01427-w.

Cromwell, H.C., Berridge, K.C., 1993. Where does damage lead to enhanced food aversion: the ventral pallidum/substantia innominata or lateral hypothalamus? Brain Res. 624, 1–10. https://doi.org/10.1016/0006-8993(93)90053-P.

Cryan, J.F., Page, M.E., Lucki, I., 2002. Noradrenergic lesions differentially alter the antidepressant-like effects of reboxetine in a modified forced swim test. Eur. J. Pharmacol. 436, 197–205. https://doi.org/10.1016/S0014-2999(01)01628-4.

Cryan, J.F., Valentino, R.J., Lucki, I., 2005. Assessing substrates underlying the behavioral effects of antidepressants using the modified rat forced swimming test. Neurosci. Biobehav. Rev. 29, 547–569. https://doi.org/10.1016/j.neubiorev.2005.03.008.

Dawbarn, D., Allen, S.J., Semenenko, F.M., 1988. Coexistence of choline acetyltransferase and nerve growth factor receptors in the rat basal forebrain. Neurosci. Lett. 94, 138–144. https://doi.org/10.1016/0304-3940(88)90284-4.

Detke, M.J., Rickels, M., Lucki, I., 1995. Active behaviors in the rat forced swimming test differentially produced by serotonergic and noradrenergic antidepressants. Psychopharmacology 121, 66–72. https://doi.org/10.1007/BF02245592.

Djordjevic, J., Djordjevic, A., Adzic, M., Radojcic, M.B., 2012. Effects of chronic social isolation on Wistar rat behavior and brain plasticity markers. Neuropsychobiology 66, 112–119. https://doi.org/10.1159/000338605.

Do, J.P., Xu, M., Lee, S.-H., Chang, W.-C., Zhang, S., Chung, S., Yung, T.J., Fan, J.L., Miyamichi, K., Luo, L., Dan, Y., 2016. Cell type-specific long-range connections of basal forebrain circuit. Elife 5. https://doi.org/10.7554/eLife.13214.

Doucette, W.T., Smedley, E.B., Ruiz-Jaquez, M., Khokhar, J.Y., Smith, K.S., 2022. Chronic chemogenetic manipulation of ventral pallidum targeted neurons in male rats fed an obesogenic diet. Brain Res. 1784, 147886 https://doi.org/10.1016/j.brainres.2022.147886.

Dulawa, S.C., Janowsky, D.S., 2019. Cholinergic regulation of mood: from basic and clinical studies to emerging therapeutics. Mol. Psychiatry 24, 694. https://doi.org/10.1038/S41380-018-0219-X.

Dwyer, T.A., Servatius, R.J., Pang, K.C.H., 2007. Noncholinergic lesions of the medial septum impair sequential learning of different spatial locations. J. Neurosci. 27, 299. https://doi.org/10.1523/JNEUROSCI.4189-06.2007.

Espinosa, N., Alonso, A., Morales, C., Espinosa, P., Chávez, A.E., Fuentealba, P., 2019. Basal forebrain gating by somatostatin neurons drives prefrontal cortical activity. Cereb. Cortex 29, 42–53. https://doi.org/10.1093/CERCOR/BHX302.

Faget, L., Zell, V., Souter, E., McPherson, A., Ressler, R., Gutierrez-Reed, N., Yoo, J.H., Dulcis, D., Hnasko, T.S., 2018. Opponent control of behavioral reinforcement by inhibitory and excitatory projections from the ventral pallidum. Nat. Commun. 9, 1–14. https://doi.org/10.1038/s41467-018-03125-y.

Farrell, M.R., Esteban, J.S.D., Faget, L., Floresco, S.B., Hnasko, T.S., Mahler, S.V., 2021. Ventral pallidum GABA neurons mediate motivation underlying risky choice. J. Neurosci. 41, 4500–4513. https://doi.org/10.1523/JNEUROSCI.2039-20.2021.

Feiro, O., Gould, T.J., 2005. The interactive effects of nicotinic and muscarinic cholinergic receptor inhibition on fear conditioning in young and aged C57BL/6 mice. Pharmacol. Biochem. Behav. 80, 251–262. https://doi.org/10.1016/J.PBB.2004.11.005.

Figueredo, L.Z.P., Moreira, K.M., Ferreira, T.L., Fornari, R.V., Oliveira, M.G.M., 2008. Interaction between glutamatergic-NMDA and cholinergic-muscarinic systems in classical fear conditioning. Brain Res. Bull. 77, 71–76. https://doi.org/10.1016/J.BRAINRESBULL.2008.05.008.

Forcelli, P.A., West, E.A., Murnen, A.T., Malkova, L., 2012. Ventral pallidum mediates amygdala-evoked deficits in prepulse inhibition. Behav. Neurosci. 126, 290–300. https://doi.org/10.1037/A0026898.

Fornari, R.V., Moreira, K.M., Oliveira, M.G.M., 2000. Effects of the selective M1 muscarinic receptor antagonist dicyclomine on emotional memory. Learn. Mem. 7, 287. https://doi.org/10.1101/LM.34900.

Freund, T.F., Antal, M., 1988. GABA-containing neurons in the septum control inhibitory interneurons in the hippocampus. Nature 336, 170–173. https://doi.org/10.1038/336170a0.

Ghosal, S., Bang, E., Yue, W., Hare, B.D., Lepack, A.E., Girgenti, M.J., Duman, R.S., 2018. Activity-dependent BDNF release is required for the rapid antidepressant actions of scopolamine. Biol. Psychiatry 83, 29. https://doi.org/10.1016/J.BIOPSYCH.2017.06.017.

Gielow, M.R., Zaborszky, L., 2017. The input-output relationship of the cholinergic basal forebrain. Cell Rep. 18, 1817–1830. https://doi.org/10.1016/J.CELREP.2017.01.060.

Gould, T.D., Dao, D.T., Kovacsics, C.E., 2009. The open field test. Neuromethods 42, 1–20. https://doi.org/10.1007/978-1-60761-303-9_1/COVER.

Gritti, I., Mainville, L., Jones, B.E., 1993. Codistribution of GABA- with acetylcholine-synthesizing neurons in the basal forebrain of the rat. J. Comp. Neurol. 329, 438–457. https://doi.org/10.1002/CNE.903290403.

Gritti, I., Manns, I.D., Mainville, L., Jones, B.E., 2003. Parvalbumin, calbindin, or calretinin in cortically projecting and GABAergic, cholinergic, or glutamatergic basal forebrain neurons of the rat. J. Comp. Neurol. 458, 11–31. https://doi.org/10.1002/cne.10505.

Gritti, I., Henny, P., Galloni, F., Mainville, L., Mariotti, M., Jones, B.E., 2006. Stereological estimates of the basal forebrain cell population in the rat, including neurons containing choline acetyltransferase, glutamic acid decarboxylase or phosphate-activated glutaminase and colocalizing vesicular glutamate transporters. Neuroscience 143, 1051–1064. https://doi.org/10.1016/j.neuroscience.2006.09.024.

Groenewegen, H.J., Berendse, H.W., Haber, S.N., 1993. Organization of the output of the ventral striatopallidal system in the rat: ventral pallidal efferents. Neuroscience 57, 113–142. https://doi.org/10.1016/0306-4522(93)90115-V.

Haber, S.N., Knutson, B., 2010. The reward circuit: linking primate anatomy and human imaging. Neuropsychopharmacology 35, 4. https://doi.org/10.1038/NPP.2009.129.

Haber, S.N., Groenewegen, H.J., Grove, E.A., Nauta, W.J.H., 1985. Efferent connections of the ventral pallidum: evidence of a dual striato pallidofugal pathway. J. Comp. Neurol. 235, 322–335. https://doi.org/10.1002/CNE.902350304.

Haj-Mirzaian, Arya, Kordjazy, N., Haj-Mirzaian, Arvin, Ostadhadi, S., Ghasemi, M., Amiri, S., Faizi, M., Dehpour, A.R., 2015. Evidence for the involvement of NMDA receptors in the antidepressant-like effect of nicotine in mouse forced swimming and tail suspension tests. Psychopharmacology 232 (19), 3551–3561. https://doi.org/10.1007/S00213-015-4004-0.

Hakan, R.L., Berg, G.I., Henriksen, S.J., 1992. Electrophysiological evidence for reciprocal connectivity between the nucleus accumbens septi and ventral pallidal region. Brain Res. 581, 344–350. https://doi.org/10.1016/0006-8993(92)90730-W.

Heimer, L., Zahm, D.S., Churchill, L., Kalivas, P.W., Wohltmann, C., 1991. Specificity in the projection patterns of accumbal core and shell in the rat. Neuroscience 41, 89–125. https://doi.org/10.1016/0306-4522(91)90202-Y.

Henny, P., Jones, B.E., 2008. Projections from basal forebrain to prefrontal cortex comprise cholinergic, GABAergic and glutamatergic inputs to pyramidal cells or interneurons. Eur. J. Neurosci. 27, 654. https://doi.org/10.1111/J.1460-9568.2008.06029.X.

Hintiryan, H., Bowman, I., Johnson, D.L., Korobkova, L., Zhu, M., Khanjani, N., Gou, L., Gao, L., Yamashita, S., Bienkowski, M.S., Garcia, L., Foster, N.N., Benavidez, N.L., Song, M.Y., Lo, D., Cotter, K.R., Becerra, M., Aquino, S., Cao, C., Cabeen, R.P., Stanis, J., Fayzullina, M., Ustrell, S.A., Boesen, T., Tugangui, A.J., Zhang, Z.-G., Peng, B., Fanselow, M.S., Golshani, P., Hahn, J.D., Wickersham, I.R., Ascoli, G.A., Zhang, L.I., Dong, H.-W., 2021. Connectivity characterization of the mouse basolateral amygdalar complex. Nat. Commun. 12, 2859. https://doi.org/10.1038/s41467-021-22915-5.

Ho, C.Y., Berridge, K.C., 2013. An orexin hotspot in ventral pallidum amplifies hedonic 'liking' for sweetness. Neuropsychopharmacology 38 (9), 1655–1664. https://doi.org/10.1038/npp.2013.62.

Jiang, L., Kundu, S., Lederman, J.D.D., López-Hernández, G.Y.Y., Ballinger, E.C.C., Wang, S., Talmage, D.A.A., Role, L.W.W., 2016. Cholinergic signaling controls conditioned-fear behaviors and enhances plasticity of cortical-amygdala circuits. Neuron 90, 1057. https://doi.org/10.1016/J.NEURON.2016.04.028.

Kiss, J., McGovern, J., Patel, A.J., 1988. Immunohistochemical localization of cells containing nerve growth factor receptors in the different regions of the adult rat forebrain. Neuroscience 27, 731–748. https://doi.org/10.1016/0306-4522(88)90179-0.

Knowland, D., Lilascharoen, V., Pacia, C.P., Shin, S., Wang, E.H.J., Lim, B.K., 2017. Distinct ventral Pallidal neural populations mediate separate symptoms of depression. Cell 170, 284–297.e18. https://doi.org/10.1016/J.CELL.2017.06.015.

Knox, D., 2016. The role of basal forebrain cholinergic neurons in fear and extinction memory. Neurobiol. Learn. Mem. 133, 39. https://doi.org/10.1016/J.NLM.2016.06.001.

Kodsi, M.H., Swerdlow, N.R., 1995. Ventral pallidal GABA-A receptors regulate prepulse inhibition of acoustic startle. Brain Res. 684, 26–35. https://doi.org/10.1016/0006-8993(95)00372-W.

Kodsi, M.H., Swerdlow, N.R., 1997. Regulation of prepulse inhibition by ventral pallidal projections. Brain Res. Bull. 43, 219–228. https://doi.org/10.1016/S0361-9230(96)00440-6.

Lehr, M.R., 2022. Impact of Adolescent Social Isolation on Ventral Pallidal Dopamine Transmission and Aversion-Resistant Drinking. Binghamton University State University of New York, United States, New York.

Mascagni, F., McDonald, A.J., 2009. Parvalbumin-immunoreactive neurons and GABAergic neurons of the basal forebrain project to the rat basolateral amygdala. Neuroscience 160, 805. https://doi.org/10.1016/J.NEUROSCIENCE.2009.02.077.

Mathis, A., Mamidanna, P., Cury, K.M., Abe, T., Murthy, V.N., Mathis, M.W., Bethge, M., 2018. DeepLabCut: markerless pose estimation of user-defined body parts with deep learning. Nat. Neurosci. 21, 1281–1289. https://doi.org/10.1038/s41593-018-0209-y.

Mcdonald, A.J., Muller, J.F., Mascagni, F., 2011. Postsynaptic targets of Gabaergic basal forebrain projections to the basolateral amygdala. Neuroscience 183, 144–159. https://doi.org/10.1016/j.neuroscience.2011.03.027.

McDonald, A.J., Mascagni, F., Zaric, V., 2012. Subpopulations of somatostatin-immunoreactive non-pyramidal neurons in the amygdala and adjacent external capsule project to the basal forebrain: evidence for the existence of GABAergic projection neurons in the cortical nuclei and basolateral nuclear com. Front. Neural Circuits 6, 46. https://doi.org/10.3389/fncir.2012.00046.

Mineur, Y.S., Obayemi, A., Wigestrand, M.B., Fote, G.M., Calarco, C.A., Li, A.M., Picciotto, M.R., 2013. Cholinergic signaling in the hippocampus regulates social stress resilience and anxiety- and depression-like behavior. Proc. Natl. Acad. Sci. U. S. A. 110, 3573–3578. https://doi.org/10.1073/PNAS.1219731110/-/DCSUPPLEMENTAL.

Moaddab, M., Ray, M.H., McDannald, M.A., 2021. Ventral pallidum neurons dynamically signal relative threat. Commun. Biol. 4 (4), 1–14. https://doi.org/10.1038/s42003-020-01554-4.

Mogenson, G.J., Jones, D.L., Yim, C.Y., 1980. From motivation to action: functional interface between the limbic system and the motor system. Prog. Neurobiol. 14, 69–97. https://doi.org/10.1016/0301-0082(80)90018-0.

Molendijk, M.L., de Kloet, E.R., 2015. Immobility in the forced swim test is adaptive and does not reflect depression. Psychoneuroendocrinology 62, 389–391. https://doi.org/10.1016/J.PSYNEUEN.2015.08.028.

Molendijk, M.L., de Kloet, E.R., 2019. Coping with the forced swim stressor: current state-of-the-art. Behav. Brain Res. 364, 1–10. https://doi.org/10.1016/J.BBR.2019.02.005.

Morais-Silva, G., Campbell, R.R., Nam, H., Basu, M., Pagliusi, M., Fox, M.E., Chan, C.S., Iñiguez, S.D., Ament, S., Cramer, N., Marin, M.T., Lobo, M.K., 2023. Molecular, circuit, and stress response characterization of ventral pallidum Npas1-neurons. J. Neurosci. 43 (3), 405. https://doi.org/10.1523/JNEUROSCI.0971-22.2022.

Morris, R., 1984. Developments of a water-maze procedure for studying spatial learning in the rat. J. Neurosci. Methods 11, 47–60. https://doi.org/10.1016/0165-0270(84)90007-4.

Navarria, A., Wohleb, E.S., Voleti, B., Ota, K.T., Dutheil, S., Lepack, A.E., Dwyer, J.M., Fuchikami, M., Becker, A., Drago, F., Duman, R.S., 2015. Rapid antidepressant actions of scopolamine: role of medial prefrontal cortex and M1-subtype muscarinic acetylcholine receptors. Neurobiol. Dis. 82, 254. https://doi.org/10.1016/J.NBD.2015.06.012.

Nusslock, R., Alloy, L.B., 2017. Reward processing and mood-related symptoms: an RDoC and translational neuroscience perspective. J. Affect. Disord. 216, 3. https://doi.org/10.1016/J.JAD.2017.02.001.

Ottenheimer, D.J., Bari, B.A., Sutlief, E., Fraser, K.M., Kim, T.H., Richard, J.M., Cohen, J.Y., Janak, P.H., 2020. A quantitative reward prediction error signal in the ventral pallidum. Nat. Neurosci. 23 (10), 1267–1276. https://doi.org/10.1038/s41593-020-0688-5.

Pang, K.C.H., Nocera, R., Secor, A.J., Yoder, R.M., 2001. GABAergic septohippocampal neurons are not necessary for spatial memory. Hippocampus 11, 814–827. https://doi.org/10.1002/HIPO.1097.

Paxinos, G., Watson, C., 2007. The Rat Brain in Stereotaxic Coordinates.

Pellow, S., Chopin, P., File, S.E., Briley, M., 1985. Validation of open : closed arm entries in an elevated plus-maze as a measure of anxiety in the rat. J. Neurosci. Methods 14, 149–167. https://doi.org/10.1016/0165-0270(85)90031-7.

Phillipson, O.T., Griffiths, A.C., 1985. The topographic order of inputs to nucleus accumbens in the rat. Neuroscience 16, 275–296. https://doi.org/10.1016/0306-4522(85)90002-8.

Pierce, R.C., Kumaresan, V., 2006. The mesolimbic dopamine system: the final common pathway for the reinforcing effect of drugs of abuse? Neurosci. Biobehav. Rev. 30, 215–238. https://doi.org/10.1016/J.NEUBIOREV.2005.04.016.

Porsolt, R.D., Anton, G., Blavet, N., Jalfre, M., 1978. Behavioural despair in rats: a new model sensitive to antidepressant treatments. Eur. J. Pharmacol. 47, 379–391. https://doi.org/10.1016/0014-2999(78)90118-8.

Richard, J.M., Ambroggi, F., Janak, P.H., Fields, H.L., 2016. Ventral pallidum neurons encode incentive value and promote cue-elicited instrumental actions. Neuron 90, 1165–1173. https://doi.org/10.1016/J.NEURON.2016.04.037/ATTACHMENT/060FFFBE-975C-4475-90FA-9439C4941B99/MMC1.PDF.

Roland, J.J., Stewart, A.L., Janke, K.L., Gielow, M.R., Kostek, J.A., Savage, L.M., Servatius, R.J., Pang, K.C.H., 2014. Medial septum-diagonal band of Broca (MSDB) GABAergic regulation of hippocampal acetylcholine efflux is dependent on cognitive demands. J. Neurosci. 34, 506–514. https://doi.org/10.1523/JNEUROSCI.2352-13.2014.

Root, D.H., Melendez, R.I., Zaborszky, L., Napier, T.C., 2015. The ventral pallidum: subregion-specific functional anatomy and roles in motivated behaviors. Prog. Neurobiol. 130, 29. https://doi.org/10.1016/J.PNEUROBIO.2015.03.005.

Rudy, J.W., 1996. Scopolamine administered before and after training impairs both contextual and auditory-cue fear conditioning. Neurobiol. Learn. Mem. 65, 73–81. https://doi.org/10.1006/NLME.1996.0008.

Saga, Y., Richard, A., Sgambato-Faure, V., Hoshi, E., Tobler, P.N., Tremblay, L., 2017. Ventral pallidum encodes contextual information and controls aversive behaviors. Cereb. Cortex 27, 2528–2543. https://doi.org/10.1093/CERCOR/BHW107.

Schindelin, J., Arganda-Carreras, I., Frise, E., Kaynig, V., Longair, M., Pietzsch, T., Preibisch, S., Rueden, C., Saalfeld, S., Schmid, B., Tinevez, J.-Y., White, D.J., Hartenstein, V., Eliceiri, K., Tomancak, P., Cardona, A., 2012. Fiji: an open-source platform for biological-image analysis. Nat. Methods 9, 676–682. https://doi.org/10.1038/nmeth.2019.

Schwarz, L.A., Luo, L., 2015. Organization of the Locus Coeruleus-Norepinephrine System. Curr. Biol. 25, R1051–R1056. https://doi.org/10.1016/j.cub.2015.09.039.

Skirzewski, M., López, W., Mosquera, E., Betancourt, L., Catlow, B., Chiurillo, M., Loureiro, N., Hernández, L., Rada, P., 2011. Enhanced GABAergic tone in the ventral pallidum: memory of unpleasant experiences? Neuroscience 196, 131–146. https://doi.org/10.1016/J.NEUROSCIENCE.2011.08.058.

Slattery, D.A., Cryan, J.F., 2012. Using the rat forced swim test to assess antidepressant-like activity in rodents. Nat. Protoc. 7, 1009–1014. https://doi.org/10.1038/nprot.2012.044.

Small, K.M., Nunes, E., Hughley, S., Addy, N.A., 2016. Ventral tegmental area muscarinic receptors modulate depression and anxiety-related behaviors in rats. Neurosci. Lett. 616, 80. https://doi.org/10.1016/J.NEULET.2016.01.057.

Smith, K.S., Berridge, K.C., 2005. The ventral pallidum and hedonic reward: neurochemical maps of sucrose "liking" and food intake. J. Neurosci. 25, 8637–8649. https://doi.org/10.1523/JNEUROSCI.1902-05.2005.

Smith, K.S., Tindell, A.J., Aldridge, J.W., Berridge, K.C., 2009. Ventral pallidum roles in reward and motivation. Behav. Brain Res. 196, 155–167. https://doi.org/10.1016/J.BBR.2008.09.038.

Soares, J.C.K., Fornari, R.V., Oliveira, M.G.M., 2006. Role of muscarinic M1 receptors in inhibitory avoidance and contextual fear conditioning. Neurobiol. Learn. Mem. 86, 188–196. https://doi.org/10.1016/J.NLM.2006.02.006.

Stephenson-Jones, M., 2019. Pallidal circuits for aversive motivation and learning. Curr. Opin. Behav. Sci. 26, 82–89. https://doi.org/10.1016/J.COBEHA.2018.09.015.

Stephenson-Jones, M., Bravo-Rivera, C., Ahrens, S., Furlan, A., Xiao, X., Fernandes-Henriques, C., Li, B., 2020. Opposing contributions of GABAergic and glutamatergic ventral pallidal neurons to motivational behaviors. Neuron 105, 921–933.e5. https://doi.org/10.1016/J.NEURON.2019.12.006.

Swerdlow, N.R., Braff, D.L., Geyer, M.A., 1990. GABAergic projection from nucleus accumbers to ventral pallidum mediates dopamine-induced sensorimotor gating deficits of acoustic startle in rats. Brain Res. 532, 146–150. https://doi.org/10.1016/0006-8993(90)91754-5.

Takatsu-Coleman, A.L., Patti, C.L., Zanin, K.A., Zager, A., Carvalho, R.C., Borçoi, A.R., Ceccon, L.M.B., Berro, L.F., Tufik, S., Andersen, M.L., Frussa-Filho, R., 2013. Short-term social isolation induces depressive-like behaviour and reinstates the retrieval of an aversive task: mood-congruent memory in male mice? J. Psychiatry Neurosci. 38, 259. https://doi.org/10.1503/jpn.120050.

Taylor, S.R., Badurek, S., Dileone, R.J., Nashmi, R., Minichiello, L., Picciotto, M.R., 2014. GABAergic and glutamatergic efferents of the mouse ventral tegmental area. J. Comp. Neurol. 522, 3308–3334. https://doi.org/10.1002/CNE.23603.

Torres, E.M., Perry, T.A., Blokland, A., Wilkinson, L.S., Wiley, R.G., Lappi, D.A., Dunnett, S.B., 1994. Behavioural, histochemical and biochemical consequences of selective immunolesions in discrete regions of the basal forebrain cholinergic system. Neuroscience 63, 95–122. https://doi.org/10.1016/0306-4522(94)90010-8.

Tóth, K., Freund, T.F., Miles, R., 1997. Disinhibition of rat hippocampal pyramidal cells by GABAergic afferents from the septum. J. Physiol. 500 (Pt 2, 463–474. https://doi.org/10.1113/jphysiol.1997.sp022033.

Unal, G., 2021. Chapter 8 - social isolation as a laboratory model of depression. In: Moustafa, A.A. (Ed.), Mental Health Effects of COVID-19. Academic Press, pp. 133–151. https://doi.org/10.1016/B978-0-12-824289-6.00005-2.

Unal, G., Canbeyli, R., 2019. Psychomotor retardation in depression: a critical measure of the forced swim test. Behav. Brain Res. 372, 112047 https://doi.org/10.1016/j.bbr.2019.112047.

Unal, G., Moustafa, A.A., 2021. The neural substrates of different depression symptoms: Animal and human studies. In: The Nature of Depression. Academic Press, pp. 59–79. https://doi.org/10.1016/B978-0-12-817676-4.00004-3.

Unal, G., Joshi, A., Viney, T.J., Kis, V., Somogyi, P., 2015a. Synaptic targets of medial septal projections in the hippocampus and extrahippocampal cortices of the mouse. J. Neurosci. 35, 15812–15826. https://doi.org/10.1523/JNEUROSCI.2639-15.2015.

Unal, C.T., Pare, D., Zaborszky, L., 2015b. Impact of basal forebrain cholinergic inputs on basolateral amygdala neurons. J. Neurosci. 35, 853–863. https://doi.org/10.1523/JNEUROSCI.2706-14.2015.

Unal, G., Crump, M.G., Viney, T.J., Eltes, T., Katona, L., Klausberger, T., Somogyi, P., 2018. Spatio-temporal specialization of GABAergic septo-hippocampal neurons for rhythmic network activity. Brain Struct. Funct. 223, 2409–2432. https://doi.org/10.1007/s00429-018-1626-0.

Vorhees, C.V., Williams, M.T., 2006. Morris water maze: procedures for assessing spatial and related forms of learning and memory. Nat. Protoc. 1, 848–858. https://doi.org/10.1038/nprot.2006.116.

Watson, C., Paxinos, G., Puelles, L., 2012. The mouse nervous. System. https://doi.org/10.1016/C2009-0-00185-8.

Wilson, M.A., Fadel, J.R., 2017. Cholinergic regulation of fear learning and extinction. J. Neurosci. Res. 95, 836. https://doi.org/10.1002/JNR.23840.

Woolf, N.J., Butcher, L.L., 1982. Cholinergic projections to the basolateral amygdala: a combined Evans blue and acetylcholinesterase analysis. Brain Res. Bull. 8, 751–763. https://doi.org/10.1016/0361-9230(82)90102-2.

Wulff, A.B., Tooley, J., Marconi, L.J., Creed, M.C., 2019. Ventral pallidal modulation of aversion processing. Brain Res. 1713, 62–69. https://doi.org/10.1016/J.BRAINRES.2018.10.010.

Yoder, R.M., Pang, K.C.H., 2005. Involvement of GABAergic and cholinergic medial septal neurons in hippocampal theta rhythm. Hippocampus 15, 381–392. https://doi.org/10.1002/HIPO.20062.

Young, S.L., Bohenek, D.L., Fanselow, M.S., 1995. Scopolamine impairs acquisition and facilitates consolidation of fear conditioning: differential effects for tone vs context conditioning. Neurobiol. Learn. Mem. 63, 174–180. https://doi.org/10.1006/NLME.1995.1018.

Yu, N., Song, H., Chu, G., Zhan, Xu, Liu, B., Mu, Y., Wang, J.-Z., Lu, Y., 2022. Basal forebrain cholinergic innervation induces depression-like behaviors through ventral subiculum hyperactivation. Neurosci. Bull. 2022 (1), 1–14. https://doi.org/10.1007/S12264-022-00962-2.

Záborszky, L., Léránth, Cs, Heimer, L., 1984. Ultrastructural evidence of amygdalofugal axons terminating on cholinergic cells of the rostral forebrain. Neurosci. Lett. 52, 219–225. https://doi.org/10.1016/0304-3940(84)90165-4.

Záborszky, L., Gombkoto, P., Varsanyi, P., Gielow, M.R., Poe, G., Role, L.W., Ananth, M., Rajebhosale, P., Talmage, D.A., Hasselmo, M.E., Dannenberg, H., Minces, V.H., Chiba, A.A., 2018. Specific basal forebrain–cortical cholinergic circuits coordinate cognitive operations. J. Neurosci. 38, 9446. https://doi.org/10.1523/JNEUROSCI.1676-18.2018.

Zahm, D.S., Williams, E., Wohltmann, C., 1996. Ventral striatopallidothalamic projection: IV. Relative involvements of neurochemically distinct subterritories in the ventral pallidum and adjacent parts of the rostroventral forebrain. J. Comp. Neurol. 364, 340–362. https://doi.org/10.1002/(SICI)1096-9861(19960108)364:2<340::AID-CNE11>3.0.CO;2-T.

Zhou, W.-L., Kim, K., Ali, F., Pittenger, S.T., Calarco, C.A., Mineur, Y.S., Ramakrishnan, C., Deisseroth, K., Kwan, A.C., Picciotto, M.R., 2022. Activity of a direct VTA to ventral pallidum GABA pathway encodes unconditioned reward value and sustains motivation for reward. Sci. Adv. 8, eabm5217. https://doi.org/10.1126/sciadv.abm5217.